SIMULATION TECHNIQUES AND MODELS FOR WHEEL-SOIL INTERACTION

László L. Kovács[a], Albert Peiret Gimenez[b], Daniel Holz[c] ,
Marek Teichmann[d] and József Kövecses[e]

[a]*Department of Mechanical Engineering, McGill University, Montreal, Canada, laszlo.kovacs@mcgill.ca*
[b]*Department of Mechanical Engineering, McGill University, Montreal, Canada, albert.peiret@mail.mcgill.ca*
[c]*CM Labs Simulations, Montreal, Canada, daniel.holz@cm-labs.com*
[d]*CM Labs Simulations, Montreal, Canada, marek@cm-labs.com*
[e]*Department of Mechanical Engineering, McGill University, Montreal, Canada, jozsef.kovecses@mcgill.ca*

Abstract
In this paper we particularly look at the wheel-terrain contact pair; the basic building block for vehicle terrain models. We will analyze the possible ways to model and simulate this interaction pair. The main goal of terramechanics modelling is to determine the effect of the distributed ground reaction force system on the wheel, and through that, the effect on the vehicle. From the modelling point of view we can then consider the dynamic behaviour of the wheel as the main modelling objective, and analyze the motion of the wheel relative to an absolute frame of reference. This motion is affected by the ground force system. Terramechanics approaches generally implicitly assume that the wheel can be modelled as a rigid body from the point of view of its global motion behaviour. Only with such assumption can a distributed force system be replaced by its resultants as it is typically done in wheel-terrain models. These resultants represent the force and moment components related to traction, compaction, side force, and motion resistance, for example. We will describe and analyze a range of possibilities of how these resultants can be determined and interpreted to represent the distributed force system and include the information about the material constitution of the ground into the model. We will present detailed implementation studies and simulation results by using semi-empirical and experimental terramechanics models, and evaluate the different approaches.

Keywords: terramechanics modelling, wheel-soil interaction, simulation

1. Introduction

The wheel forms the main interface between a vehicle and its environment, and modelling the wheel-terrain interaction is one of the most challenging problems in the dynamics simulation of off-road vehicles. The complexity of this stems from modelling the soil reactions at different driving conditions and balancing between accuracy and computational cost.

In general, interaction models with finite element discretization, or the discrete element model based representation of the soil, require less modelling assumptions [1, 2]. On the other hand, these models do not allow for real time simulation, and the time required for simulating a vehicle limits their use in current engineering practice. For mobility/trafficability analysis, the semi-empirical Bekker [3] and Wong-Reece models [4, 5, 6], and such experimen-

tal models [7, 8, 9] are preferred which can support statistical analysis [10]. In the formulations proposed by Bekker, and imporved by Wong and Reece, the normal stress distribution is typically determined based on an empirical model, while the shear stresses are calculated analytically by using the kinematics of the wheel and applying the Janosi-Hanamoto formula [11]. Then the resultant ground reaction forces and moments applied to the wheel are calculated by the integration of these stresses along the contact patch. Although these models can give a good estimate on the steady state wheel-soil interaction behaviour in certain motion regimes (typically for higher slip ratios), they do not take into account the soil profile, the soil dynamics or the transient motion of the wheel. Similarly, the traction prediction equations obtained through the statistical analysis of a large number of experiment are only valid for steady state conditions. These model however may embed extra information on the tire effects without the need of considering the actual contact patch and tire deformation.

None of the above classical terramechanics models include information on the dynamics of the wheel-soil contact pair, and they have limitations regarding the vertical dynamics. The pressure-sinkage relationship of the Bekker model is based on quasi-static experimental results. The Wong-Reece model modifies this relationship by including the effect of slip through considering the change of the location of the maximum normal stress at different driving conditions. This is also based purely on experimental observations made in steady state, and the proposed empirical formula may not predict accurately the stress distributions in dynamic simulations. In the experimental traction prediction formulas the cone-index [8, 4] characterizes the load bearing capability of the soil. This is used to determine the mobility or mobility reduction due to the expected sinkage of the wheel, but otherwise there is no information available on the vertical interaction force acting on the wheel.

Regarding the traction force, the Wong-Reece model assumes that the flow of the soil under the wheel can be neglected for driven wheels, while an average soil velocity is considered for towed wheels [6]. These assumptions results in different shear stress distributions which are in better agreement with the experiments. It was also pointed out in [12] that considering the resultant traction force as a concentrated force acting at the very bottom of the rigid wheel may require case specific considerations for the corresponding contact velocity. This is due to the fact the forward flow of the soil cannot be neglected during braking and it has to be accounted for even in case of models that use the resultant force and moments originating from terramechanics relations.

The inaccuracies in the modelling of the stress distributions in case of the semi-empirical models are partially compensated by the fact that the resultant forces and moments that are acting on the wheel are calculated by integration. Therefore, they provide a good approximation for simulating steady state behaviour and can be used to qualitatively simulate the wheel-soil interaction. For quantitative agreements case specific corrections, tuning and further improvement of the models might be necessary [2, 13].

The steady state assumptions, the insufficient data in some operating regimes (e.g., braking), and/or unavailable soil properties demand for robust simulation methods. Therefore, in the present paper, we will apply a constraint-based complementarity formulation [12] for the dynamic simulation of the wheel-soil contact pair. This previous work is further developed, and applied to not only the semi-empirical Wong-Reece model, but to two other examples using cone-index based traction prediction equations. The focus of our analysis is on the applicability of the steady state models in dynamic simulation with real time requirements. The chosen examples will also allow us to show the different possible interpretation of the ground reaction components and their consideration in dynamic simulations.

2. Wheel-Soil interaction models

The wheel-soil interaction may be modelled by considering the soil as a continuum, or as a granular material. Also, for wheels with tire, the flexibility of the tire may be modelled by lumped viscoelastic elements or by using a continuum based description. Whether a discretized model or a continuum model is more appropriate for analysing a given problem depends on many factors. These could include the accessible computational tools, the availability of soil properties, the expected simulation time and precision. Very often, the wheel is modelled as a rigid body and the soil is considered as a continuum. In these cases the soil reactions are determined by integrating the shear and normal stresses acting at the wheel-soil interface. Another approach is to set up a model is to use a large number of experiments and preform dimensional analysis. The traction prediction equations obtained this way are based entirely on experimental observations, and generally have only a few parameters that characterize the mobility of a vehicle based on the load bearing capability of the soil, tire deflection and wheel geometry.

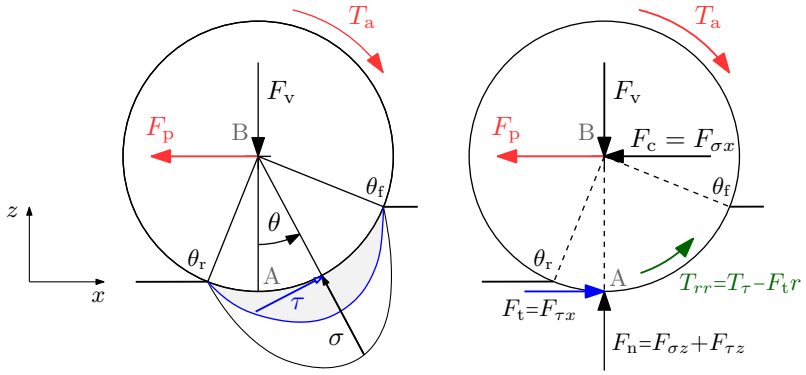

Fig. 1. Equivalent force system corresponding to the Wong-Reece model

2.1 Semi-empirical models

The semi-empirical models consider the soil as continuum and use experimental data as well as the kinematics of the wheel to approximate the stress distributions under the wheel. The pressure sinkage formula [3, 5] that determines the normal stresses have the general form

$$\sigma = (k_1 + k_2\, b) \left(\frac{\zeta(\theta, \theta_m)}{b} \right)^n \tag{1}$$

where k_1, k_2 are soil properties, and $\zeta(\theta, \theta_m)$ is the sinkage of a point on the perimeter of the wheel located by angle θ and modified according to the known location, θ_m, of the maximum normal stress. This location may also depend on the slip, i_s, and the properties of the soil. In addition, parameter b is the characteristic size (width) of the wheel, and n is the sinkage exponent.

The kinematics of the wheel is considered to determine the shear deformation along the perimeter of the wheel. For this, it is usually assumed that both the angular and the linear velocity of the wheel is constant. Then, by approximating the shape of the stress-deformation curve, the shear stresses may be calculated by the bounded exponential formula [11]

$$\tau = (c + \sigma \tan\phi) \mathrm{e}^{-j(\theta, i_s)/K} \tag{2}$$

where c and ϕ are the cohesion and the internal friction angle of the soil, K is the shear deformation modulus, and $j(\theta, i_s)$ is the shear deformation. In the expression of the shear deformation the dots indicate that its calculation depends also on other factors, like the assumption made on the soil flow under different driving conditions [5, 6].

By using the stresses defined in Eqs. (1) and (2) the resultant force system acting at the centre of a wheel can be written as

$$F_x = F_{\tau x} - F_{\sigma x} = rb \int_{\theta_r}^{\theta_f} \tau \cos\theta \, \mathrm{d}\theta - rb \int_{\theta_r}^{\theta_f} \sigma \sin\theta \, \mathrm{d}\theta \tag{3}$$

$$F_z = F_{\tau z} + F_{\sigma z} = rb \int_{\theta_r}^{\theta_f} \tau \sin\theta \, \mathrm{d}\theta + rb \int_{\theta_r}^{\theta_f} \sigma \cos\theta \, \mathrm{d}\theta \tag{4}$$

$$T_y = -T_\tau = -r^2 b \int_{\theta_r}^{\theta_f} \tau \, \mathrm{d}\theta \tag{5}$$

where θ_f and θ_r are the front and rear contact angles, r is the radius of the wheel, and the subscripts $_\sigma$ and $_\tau$ refer to force components that are due to the normal and shear stresses, respectively. Coordinate x denotes the longitudinal motion direction and z points normal to the ground. Generally, infinitely many other equivalent force systems could be considered. However, when one wants to analyze the wheel-soil interaction, it is advantageous to consider such an equivalent force system the components of which directly define the normal force and the traction force [12], for example. A possible choice of an equivalent system of generalized forces is shown in Fig. 1, where F_n is the normal force, F_t is the traction force, F_c is the resistance force due to soil compaction, and T_{rr} is the residual resistance torque corresponding to shearing. These components are defined as

$$F_n = F_{\tau z} + F_{\sigma z}\,, \quad F_t = F_{\tau x}\,, \quad F_c = F_{\sigma x} \quad \text{and} \quad T_{rr} = T_\tau - F_t r \tag{6}$$

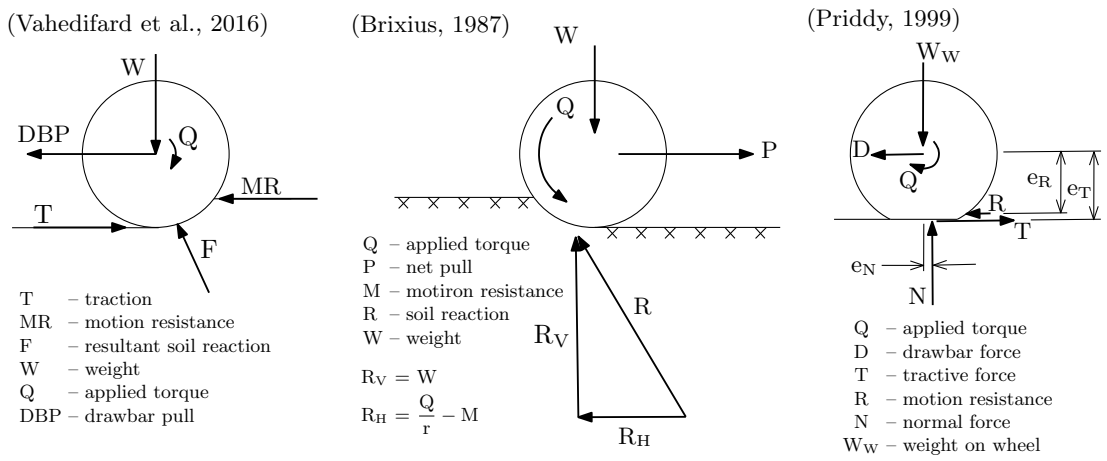

Fig. 2. Equivalent force systems considered in experimental models (reproduced based on [8], [14] and [15])

This set of generalized forces constitute to a physically motivated selection of the interaction force components. We also note that these components form a non-minimum set of generalized forces. For example, the longitudinal/horizontal components F_t and F_c could not be measured separately in an experiment.

2.2 Experimental models

The experimental models focus on expressing the drawbar pull, i.e., the pulling force a wheel can exert, as function of the slip ratio and other parameters characterizing the mobility of a vehicle. This force can directly be measured or calculated from measurements. Similarly, the motor torque is a quantity which can be measured, and the motion resistance can then be calculated as the difference of the thrust provided by this torque and the drawbar pull.

By using the traction prediction formulas proposed in [8], the steady state relationship can be written as

$$\frac{Q}{r} = P + M \tag{7}$$

where P is the pull, M is and the motion resistance, Q/r is the thrust, which is assumed to be proportional to the applied torque in steady state Q. The model predictions for the torque ratio and the motion resistance ratio are

$$\frac{Q}{rW} = 0.88\left(1-\mathrm{e}^{-0.1B_\mathrm{n}}\right)\left(1-\mathrm{e}^{-7.5i_\mathrm{s}}\right)+0.04 \tag{8}$$

$$\frac{M}{W} = \frac{1}{B_\mathrm{n}} + \frac{0.5i_\mathrm{s}}{\sqrt{B_\mathrm{n}}} + 0.04 \tag{9}$$

where i_s is the slip, W is the weight (vertical load on the wheel) and B_n is the mobility number. This mobility number primarily depends on the cone index (CI) which characterizes the load bearing capability of the soil.

While the pull, the thrust and the motion resistance are the main force components used in the literature, their interpretation might be different due to how the corresponding equivalent force systems are considered. For example, as it is shown in Fig. 2 the motion resistance is sometimes represented as a force acting at the "surface" of the soil, which choice is arbitrary.

As it was stated above, in the present work we use a constraint based complementarity formulation to simulate the wheel. In this formulation it is essential to define the contact velocities that corresponds to the ground reaction components. For this, we propose to use the same equivalent force system that was presented for the Wong-Reece model in Fig. 1, but assign different meaning to each components. In this figure, the pull is denoted by F_p, and T_a is the applied torque, but the traction force and the compaction resistance can have two different interpretations.

One possibility is to model the motion resistance as a force applied at the centre of the wheel. In this case $T_\mathrm{a} = Q$, $F_\mathrm{c} = M$, and the traction force is equal to the thrust, i.e., $F_\mathrm{t} = T_\mathrm{a}/r$. From the torque balance it also follows that $T_\mathrm{rr} = 0$. In the following we will term this as the *force equivalent* model of motion resistance. Alternatively, the motion

resistance can also be interpreted as a torque with $T_{\mathrm{rr}} = Mr$ and by setting $F_{\mathrm{c}} = 0$. In this case, the traction force will be equal to the pull, $F_{\mathrm{t}} = P$. The corresponding model is called the *torque equivalent* model henceforward. We note that these models are really just different representations of the same system of forces acting on the wheel, but they might show a slightly different dynamic behaviour when they are used with the constraint-based complementarity formulation.

3. Simulation Methodology

The kinematics of vehicle systems can be represented by a set of generalized coordinates $\mathbf{q}$ and a set of generalized velocities $\mathbf{v}$, which can be related through the transformation $\dot{\mathbf{q}} = \mathbf{N}(\mathbf{q})\mathbf{v}$. Then, the dynamic equation of the system can be written as follows

$$\mathbf{M}\dot{\mathbf{v}} = \mathbf{f}_{\mathrm{a}} + \mathbf{f}_{\mathrm{g}} \tag{10}$$

where $\mathbf{M}(\mathbf{q})$ is the mass matrix, $\mathbf{f}_{\mathrm{g}}$ contains the generalized ground reaction forces, and $\mathbf{f}_0$ contains the rest of generalized forces acting on the system.

To integrate the system equations in a dynamic simulation, some considerations regarding the time discretization need to be taken. The ground reaction forces can be computed by using the state of the system at the beginning of the time-step, and applied directly on the system as known forces. In such case, this *explicit* force representation allows to determine the acceleration of the system, and the system velocity at the end on the time step can be computed using a finite difference approximation of the velocity as

$$\mathbf{v}^{k+1} = \mathbf{v}^{k} + h\mathbf{M}^{-1}\left(\mathbf{f}_{\mathrm{a}}^{k} + \mathbf{f}_{\mathrm{g}}^{k}\right) \tag{11}$$

where $\mathbf{v}^k$ and $\mathbf{v}^{k+1}$ are the velocity at the beginning and at the end of the time-step, h is the time-step size, and $\mathbf{M}$ is computed using the known configuration of the system. The configuration at the end of the time step can then be determined as

$$\mathbf{q}^{k+1} = \mathbf{q}^{k} + h\mathbf{N}\mathbf{v}^{k+1} \tag{12}$$

where $\mathbf{q}^k$ and $\mathbf{q}^{k+1}$ are the configuration at the beginning and at the end of the step. The velocity transformation matrix $\mathbf{N}$ is computed using the known state of the system.

On the other hand, the ground reaction $\mathbf{f}_{\mathrm{g}}$ can be considered as *implicit* constraint forces, so that their values in the current time-step depend on the velocity at the end of the step $\mathbf{v}^{k+1}$. For this purpose, we shall define a set of constraints to represent such forces, which can be characterized by the set of constraint velocities $\mathbf{u} = \mathbf{A}\mathbf{v}$, where $\mathbf{A}(\mathbf{q})$ is the constraint Jacobian matrix. Then, the dynamic model in Eq. (10) can be written as

$$\mathbf{M}\dot{\mathbf{v}} = \mathbf{f}_{\mathrm{a}} + \mathbf{A}^{\mathrm{T}}\boldsymbol{\lambda} \tag{13}$$

where $\boldsymbol{\lambda}$ contains the ground reaction forces that the integration scheme needs to solve for.

Following a similar approach as above, the dynamic model in (13) can be discretized via a finite difference approximation and written in matrix form as

$$\begin{bmatrix} \mathbf{M} & -\mathbf{A}^{\mathrm{T}} \\ \mathbf{A} & \mathbf{0} \end{bmatrix} \begin{bmatrix} \mathbf{v}^{k+1} \\ h\boldsymbol{\lambda}^{k+1} \end{bmatrix} = \begin{bmatrix} \mathbf{M}\mathbf{v}^{k} + h\mathbf{f}_{\mathrm{a}}^{k} \\ \mathbf{u}^{k+1} - \mathbf{u}^{\mathrm{R}} \end{bmatrix} \tag{14}$$

where $\boldsymbol{\lambda}^{k+1}$ are the unknown constraint forces, $\mathbf{u}^{k+1}$ are the unknown constraint velocities, and $\mathbf{u}^{\mathrm{R}}$ are reference velocities. However, with this many unknown variables, some additional relations need to be specified to be able to solve the dynamic equations. For this purpose, the ground reaction forces can be approximated by specifying a range of feasible values, so that each constraint velocity ($i = 1 \ldots n_u$) can be defined as

$$u_i^{k+1} \begin{cases} \geqslant u_i^{\mathrm{R}} & \\ = u_i^{\mathrm{R}} & \text{if} \quad \lambda_i^{k+1} \in \left(\lambda_i^{\mathrm{L}}, \lambda_i^{\mathrm{U}}\right) \\ \leqslant u_i^{\mathrm{R}} & \end{cases} \qquad \begin{array}{l} \lambda_i^{k+1} = \lambda_i^{\mathrm{L}} \\ \\ \lambda_i^{k+1} = \lambda_i^{\mathrm{U}} \end{array} \tag{15}$$

where u_i^{R} is usually zero, and λ_i^{L} and λ_i^{U} are the lower and upper bound of the constraint force, which are estimated based on the *desired force* $\lambda_i^{\mathrm{D}} \in \left[\lambda_i^{\mathrm{L}}, \lambda_i^{\mathrm{U}}\right]$ defined by the model and using the current state. This constraint force law

in Eq. (15), can be used to characterize many different non-smooth phenomena, such as unilateral contact, as well as Coulomb friction. Here, it is used for modelling the wheel-soil interaction forces obtained through terramechanics models.

The new configuration computed in the same way as in the explicit integration scheme, see Eq. (12). In addition, the proposed constraint-based representation can be formulated as a mixed linear complementarity problem (MLCP)

$$\mathbf{A}\mathbf{M}^{-1}\mathbf{A}^{\mathrm{T}}h\boldsymbol{\lambda}^{k+1}+\mathbf{A}\left(\mathbf{v}^{k}+h\mathbf{M}^{-1}\mathbf{f}_{\mathrm{a}}^{k}\right)+\mathbf{u}^{\mathrm{R}}=\mathbf{u}^{k+1}\quad\perp\quad\boldsymbol{\lambda}^{k+1}\in\left[\boldsymbol{\lambda}^{\mathrm{L}},\boldsymbol{\lambda}^{\mathrm{U}}\right] \tag{16}$$

where the operator $\perp$ describes the component-wise complementarity condition given in Eq. (15). If the lead matrix of the problem $\mathbf{A}\mathbf{M}^{-1}\mathbf{A}^{\mathrm{T}}$ is positive definite, the problem has a unique solution, but if it is rank deficient, there are infinitely many possible solutions. This happens when the system of ground forces applied to the wheel is redundant. In such a case, the regularization of the constraint can solve this issue by defining an additional relation between the constraint force and the constraint velocity while the force is within bounds bound, i.e., if $\lambda_i^{k+1}\in\left(\lambda_i^{\mathrm{L}},\lambda_i^{\mathrm{U}}\right)$,

$$\lambda_i^{k+1}=-d_i\left(u_i^{k+1}-u_i^{\mathrm{R}}\right) \tag{17}$$

where d_i is a damping coefficient that tends to infinity when there is no regularization, and it might be defined using the desired force λ_i^{D} and the current constraint velocity u_i^k.

4. Single wheel case study

To simulate a single wheel, we can describe its planar motion with the two velocity components of the centre v_x and v_z, and the angular velocity ω_y. The dynamic model in Eq. (10) associated with these generalized velocities has the simple form

$$\begin{bmatrix} m_x & 0 & 0\\ 0 & m_z & 0\\ 0 & 0 & I_y \end{bmatrix}\begin{bmatrix} \dot{v}_x\\ \dot{v}_z\\ \dot{\omega}_y \end{bmatrix}=\begin{bmatrix} -F_{\mathrm{p}}\\ -m_z g\\ T_{\mathrm{a}} \end{bmatrix}+\begin{bmatrix} F_x\\ F_z\\ T_y \end{bmatrix} \tag{18}$$

where F_{p} is the externally applied pull, T_{a} is the motor torque applied to the wheel, $g=9.81\,\mathrm{m/s^2}$ is the acceleration of gravity, and the ground force components F_x, F_z, and T_y are the resultant system of forces acting on the wheel. The quantities m_x and m_z describe the mass of the system associated with the horizontal and vertical directions, respectively, and I_y is the moment of inertia of the wheel about its axis.

Commonly these mass quantities take into account not only the mass of the wheel, but also the mass of part of the vehicle. The assumption that the centre of the wheel is constrained to the chassis of the vehicle is valid for the cases where the suspension system does not significantly affect the vehicle dynamics. For our study, we use a model of a *quarter-vehicle* with one single wheel.

The parameters of this model and the considered soil properties are collected in Tab. 1. The mass of the vehicle, the size of the wheel, and the soil properties are similar to the parameters used in reference [12] to simulate a planetary rover with rigid wheels. The parameters of the empirical, cone-index based model were selected independently, but the stiffness of the soil, $k_z=k_1+k_2 b$, was derived from the Wong-Reece model to have a similar vertical dynamics. In addition, p_{w} is the tire pressure and h_{w} is the section height of the wheel which are only used to calculate the mobility number B_{n} in the traction prediction equations. Otherwise the wheel is considered as rigid.

Table 1. Simulation parameters

Vehicle		Wong-Reece model				Cone index model	
m_x	116 kg	k_1	5.7 kPa	K	0.0115 m	CI	400 kPa
m_z	116 kg	k_2	2293.2 kPa/m	θ_{m}	$c_0+c_1 i_s$	k_z	116.18 kN/m
I_y	0.6245 kg m^2	n	1 –	c_0	0.2 rad	d_z	10 kN s/m
r	0.2794 m	c	1.15 kPa	c_1	0.1 rad	p_{w}	100 kPa
b	0.25 m	ϕ	0.5498 rad			h_{w}	0.1625 m

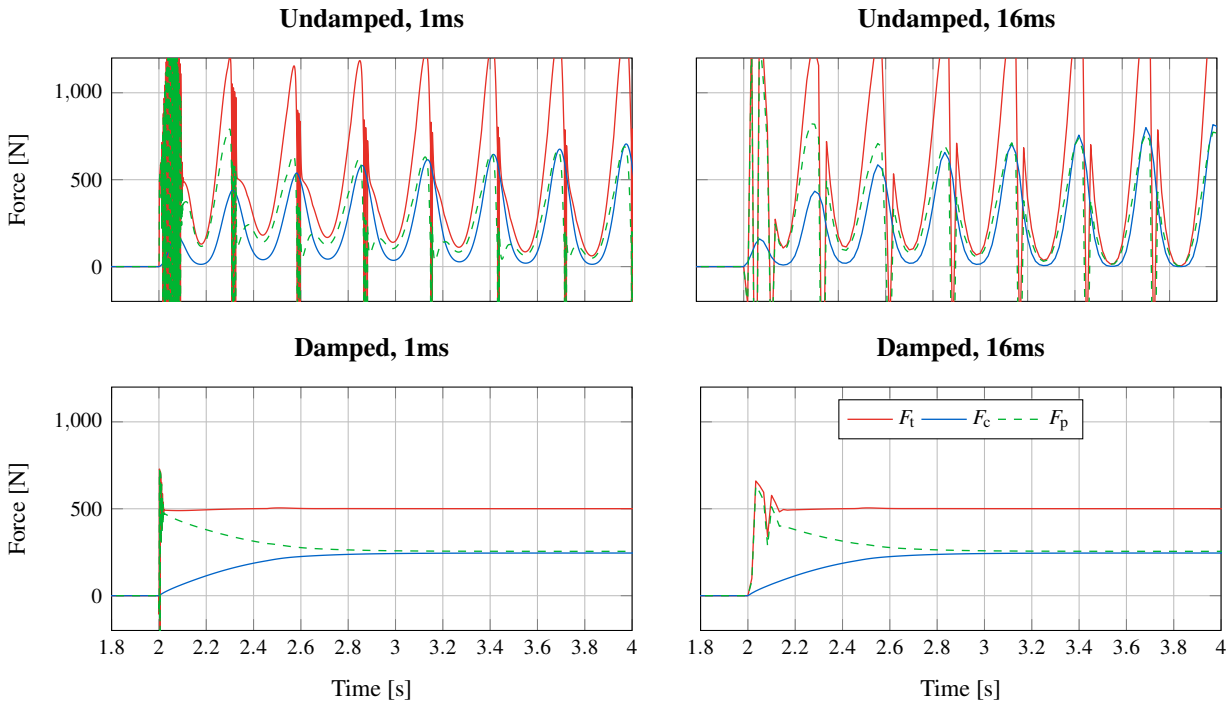

Fig. 3. Wong-Reece model simulated with explicit (direct) application of the wheel-soil interaction forces

4.1 Acceleration test example

The Wong-Reece model was simulated with the single wheel model by following the aforementioned approaches, for which a constant motor torque $T_a = 150\,\text{Nm}$ was applied in all cases, and the external pull was set to $F_p = 0$. We differentiate between *explicit* and *implicit* force representation of the ground reactions, and we use different time-step sizes (1 ms or 16 ms). Moreover, the effect of damping in the system was studied by adding damping to the vertical resultant force component with a ratio $\eta = d_z/k_z = 0.1$ s, where k_z and d_z are the stiffness and damping coefficients [12].

The direct application of the forces (explicit representation) leads to the results shown in Fig. 3. Without damping the simulation becomes unstable, and the instability is slightly stronger for larger time-step sizes. The simulation becomes stable when damping is added to the vertical dynamics, but small high-frequency oscillations may still be present at the beginning of the motion. These are filtered out (aliased) when larger time steps are used. These results show that the semi-empirical Wong-Reece model is not appropriate for dynamic simulations in its original form, because the steady state assumption leaves damping out of the model, which needs to be reintroduced in order to simulate a system under some dynamic conditions.

In the results shown in Fig. 4 the ground reactions are applied through constraint forces (implicit representation). The undamped model at 1 ms still shows an unstable behaviour. However, increasing the step size to 16 ms makes the simulation more stable due to the implicit nature of the constraint forces. Moreover, adding damping to the system helps to reduce the oscillations at the beginning. There was no regularization applied in these cases, and the effect of the regularization on the system dynamics is discussed below.

4.2 Steady state test example

To make the system reach a steady state (i.e., constant velocity), a constant pull F_p was applied throughout the simulation, and the torque applied to the wheel was kept constant at the beginning, while after reaching a certain

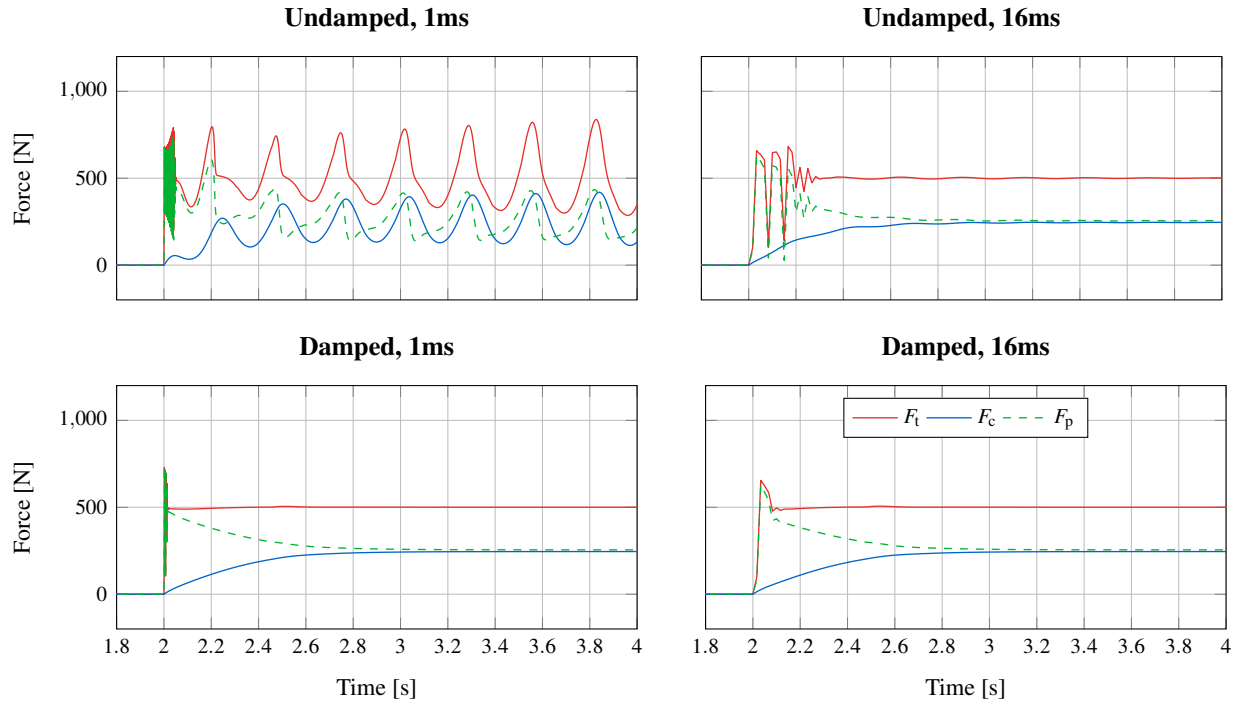

Fig. 4. Wong-Reece model simulated with implicit (constraint-based) application of the wheel-soil forces

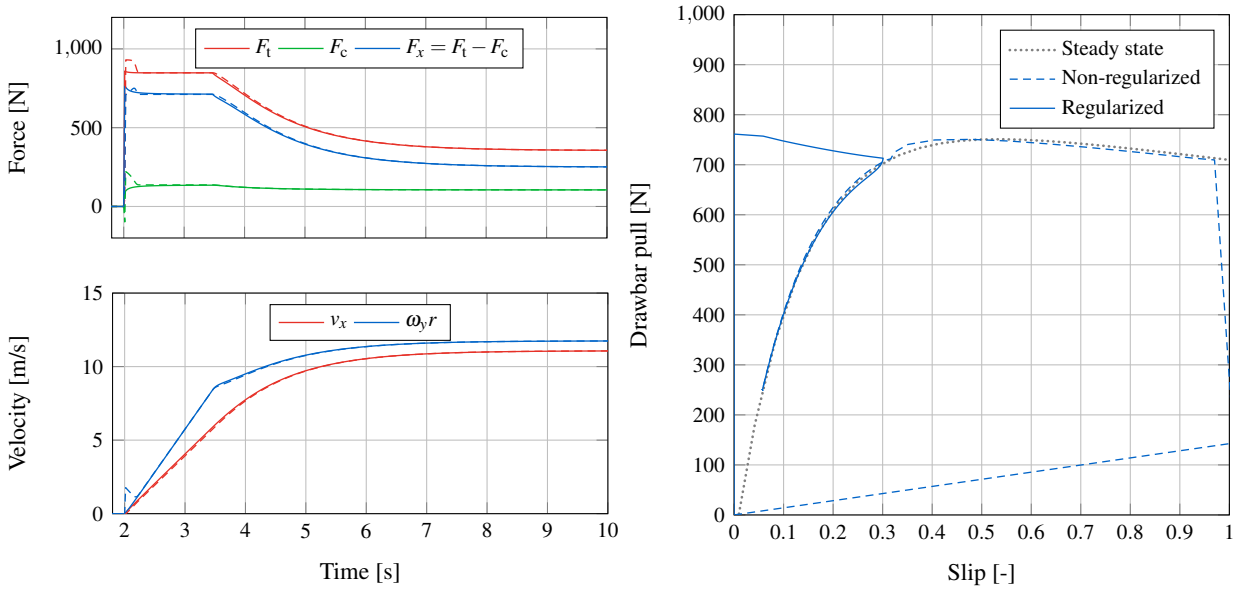

Fig. 5. Transient behaviour and steady state simulation of the force equivalent cone index model using implicit force representation with $T_{\max} = 250\,\mathrm{Nm}$ and $F_p = 250\,\mathrm{N}$

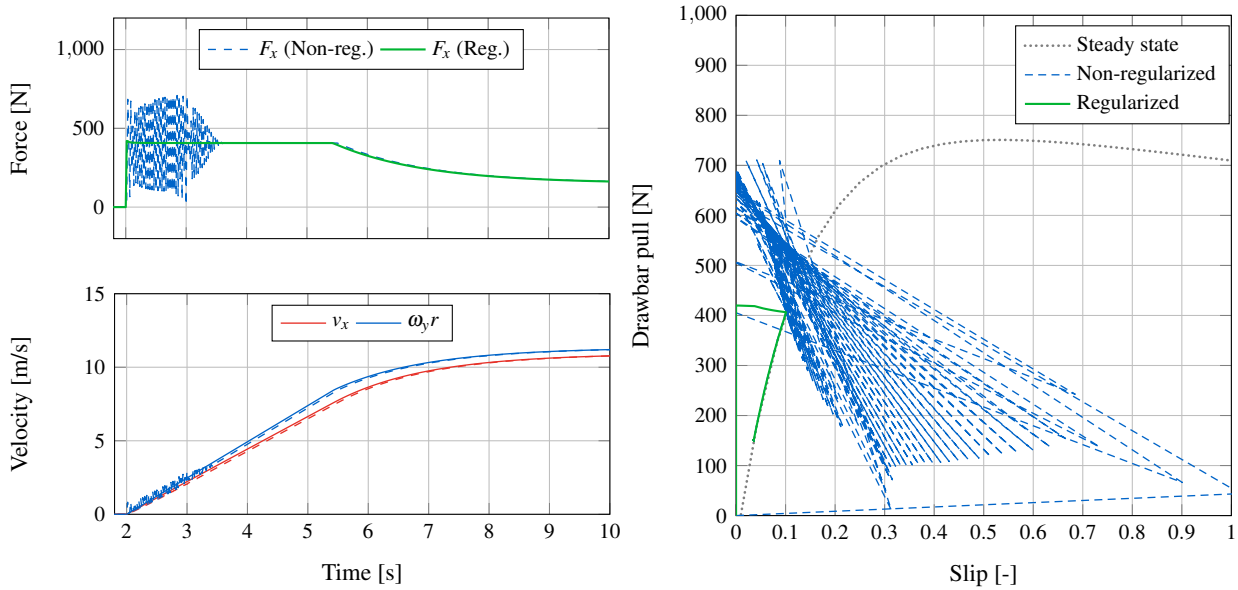

Fig. 6. Transient behaviour and steady state simulation of the torque equivalent cone index model using implicit force representation with $T_{\max} = 150\,\text{Nm}$ and $F_\text{p} = 150\,\text{N}$

angular velocity it was reduced according to the actuation law

$$T_\text{a} = \begin{cases} T_{\max} & \omega_y \leqslant \omega_{\text{sat}} \\ T_{\max}\left(\dfrac{\omega_{\max} - \omega_y}{\omega_{\max} - \omega_{\text{sat}}}\right) & \text{if} \quad \omega_y \in (\omega_{\text{sat}}, \omega_{\max}) \\ 0 & \omega_y \geqslant \omega_{\max} \end{cases} \tag{19}$$

where $T_{\max}$ is the torque applied to the wheel at the beginning of the simulation, $\omega_{\text{sat}} = 30\,\text{rad/s}$ is the angular velocity from which the applied torque starts to decrease, and $\omega_{\max} = 50\,\text{rad/s}$ is the maximum velocity from which no torque is applied. In addition, all the simulations were carried out using the implicit representation of forces (constraint-based) in order to assess the effect of the regularization on the system dynamics.

Figure 5 shows the results with the *force equivalent* cone index model, where the initial torque was set to $T_{\max} = 250\,\text{Nm}$, and the pull was $F_\text{p} = 250\,\text{N}$. As it can be seen, the system reaches a steady state, and so the forces and velocities remain constant at the end of the simulation. Moreover, the relation between the drawbar pull and the slip is satisfied when the steady state is reached. The non-regularized formulation uses $u^\text{R} = 0$, and the force bounds are set to the desired steady state force, i.e., $\lambda^\text{U} = -\lambda^L = |\lambda^\text{D}|$. Whereas, the regularized formulation uses $u^\text{R} = 0$, the force bounds are set to the maximum traction force (i.e., slip ratio $i_\text{s} = 1$), and the damping coefficient defined in Eq. (17) is $b = \lambda^\text{D}/u^k$, which acts as an adaptive damping.

Substantial differences between regularized and non-regularized forces can be appreciated at the beginning of the simulation. Without regularization, the slip ratio increases up to large slip values, and later, it is reduced until the system reaches the steady state. On the other hand, with constraint regularization, the slip ratio increases from zero until the force that is applied matches the desired force, then the torque is reduced until the steady state is reached. Both simulations reach the same steady state, but with different dynamic behaviour. To be able discuss the accuracy of these models in dynamic simulations, and determine the one that better captures the wheel-soil interaction, experimental data would be needed.

Furthermore, other conditions with lower applied torque and pull, $T_{\max} = 150\,\text{N}$ and $F_\text{p} = 150\,\text{N}$, were analysed using the torque equivalent cone index model, see Fig. 6. It is shown that simulating this system without regularization can lead to strong oscillations before reaching a steady state. Such oscillations are very much apparent for the ground reaction forces but less significant for the velocities. The regularization solves this problem, by adding the adaptive damping coefficient d, and also by increasing the force bounds to better approximate the traction force for higher slip ratios. This allows the traction force to increase when the wheel starts to move and therefore it helps to avoid the initial

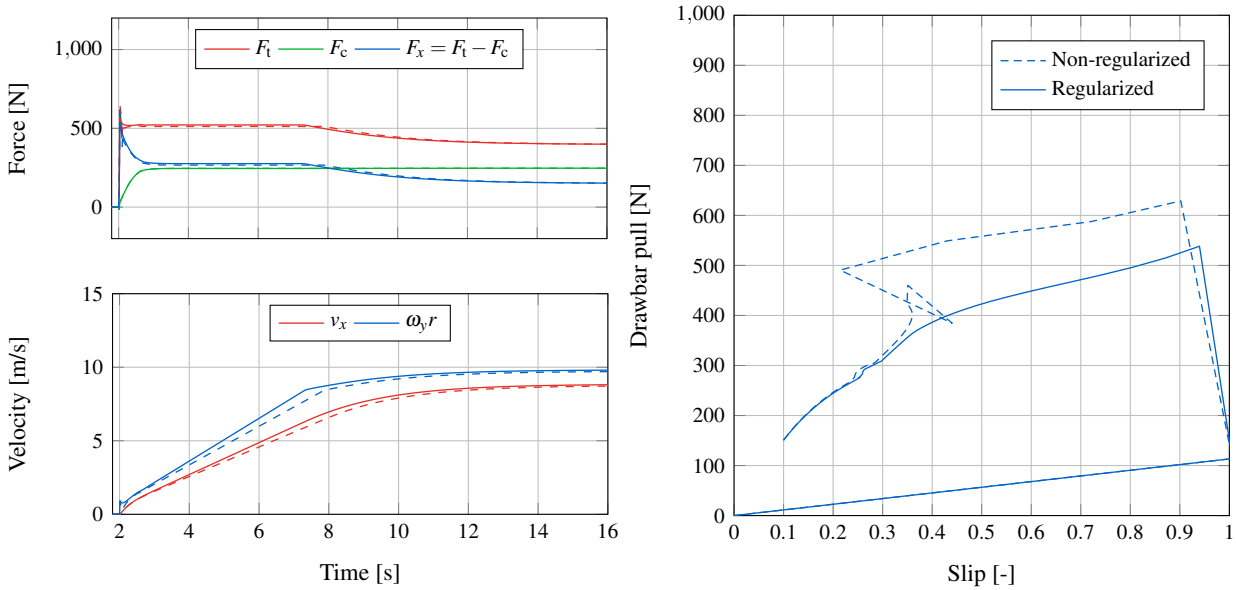

Fig. 7. Transient behaviour and steady state simulation of the Wong-Reece model using implicit force representation with $T_{\max} = 250\,\text{Nm}$ and $F_p = 250\,\text{N}$

large variations in the slip observed with the non-regularized model.

It is worth mentioning that the simulations in Figs. 5 and 6 were performed with both the force and torque equivalent models of the cone index. These to models use a different set of force components, as discussed in Section 2. However, they represent the same system of forces acting on the wheel, and so the motion of the system turns out to be the same in both cases.

Finally, the Wong-Reece model was simulated with the same input values, $T_{\max} = 150\,\text{N}$ and $F_p = 150\,\text{N}$. The corresponding results are shown in Fig. 7. Here, the upper and lower bounds of the constraint forces λ^U and λ^L are defined by the desired force in both cases, that is why the slip ratio increases up to $i_s = 1$ at the beginning. Even though the input forces are the same as in the previous simulation with the cone index, the soil properties are different, therefore giving different results. The regularized implementation does not differ much from the non-regularized one, and both reach the exact same steady state.

5. Conclusions

The modelling considerations on the wheel-soil interaction has an effect on the dynamic behaviour of vehicle systems. This may be important in simulation where the state of the system is constantly changing. Furthermore, different approaches can be followed to apply the ground reaction forces on the wheel: explicit and implicit. The explicit force representation might become unstable if no damping is added to the model. On the other hand, implicit representations lead to more robust simulations, especially in dynamic simulations where a steady state is not reached. A detailed case study was used to show how these formulations perform in the simulation of a quarter-vehicle model.

References

[1] Nakashima, H. and Oida, A., 2004. Algorithm and implementation of soiltire contact analysis code based on dynamic FEDE method, Journal of Terramechanics, **41**(2–3), 127–137.

[2] Smith, W., Melanz, D., Senatore, C., Iagnemma, K., Peng, H., 2014. Comparison of discrete element method and traditional modeling methods for steady-state wheel-terrain interaction of small vehicles, Journal of Ter-

ramechanics, **56**, 61–75.

[3] Bekker, M.G., 1956. Theory of land locomotion: the mechanics of vehicle mobility, The University of Michigan Press, Ann Arbor.

[4] Wong, J.Y., 2009. Terramechanics and off-road vehicle engineering: Terrain behaviour, Off-road vehicle performance and design, 2nd edition, Butterworth-Heinemann.

[5] Wong, J.Y., Reece, A.R., 1967. Prediction of rigid wheel performance based on the analysis of soil-wheel stresses – Part I. Performance of driven rigid wheels, Journal of Terramechanics, **4**(1), 81–98.

[6] Wong, J.Y., Reece, A.R., 1967. Prediction of rigid wheel performance based on the analysis of soil-wheel stresses – Part II. Performance of towed rigid wheels, Journal of Terramechanics, **4**(2), 7–25.

[7] Wismer, R.D., Luth, H.J., 1973. Off-road traction prediction for wheeled vehicles, Journal of Terramechanics, **10**(2), 49–61.

[8] Brixius, W.W., 1987. Traction prediction equations for bias ply tires, 87-1622, American Society of Agricultural Engineers.

[9] Williams, J.M., Vahedifard, F., Mason, G.L., Priddy, J.D., 2017. New algorithms for predicting longitudinal motion resistance of wheels on dry sand, Journal of Defense Modeling and Simulation: Applications, Methodology, Technology, Special Issue (February 2017), 1–13.

[10] McCullough, M., Jayakumar, P., Dasch, J., Gorsich, D., 2017. The Next Generation NATO Reference mobility model development, Journal of Terramechanics, textbf73, 49–60.

[11] Janosi, Z., Hanamoto, B., 1961. Proceedings of the 1st International Conference on Terrain-Vehicle Systems, The analytical determination of drawbar pull as a funcition of slip for tracked vehicle, Edizioni Minerva Tecnica, Torino, Italy, 707–736.

[12] Azimi, A., Holz, D., Kövecses, J., Angeles, J., Teichmann, M., 2015. A multibody dynamics framework for simulation of rovers on soft terrain, Journal of Computational and Nonlinear Dynamics, **10**(3), 031004.

[13] Senatore C., Iagnemma K., 2014. Analysis of stress distributions under lightweight wheeled vehicles, Journal of Terramechanics, **51**, 117.

[14] Vahedifard, F., Robinson, J.D., Mason, G.L., Howard, I.L., Priddy, J.D., 2016. Journal of Terramechanics, **63**, 13–22.

[15] Priddy J.D., 1999. Improving the Traction Prediction Capabilities in the NATO Reference Mobility Model (NRMM). Technical Report GL-99-8, US Army Corps of Engineers, Waterways Experiment Station.